

Magnetic-field-induced density of states in MgB_2 : Spin susceptibility measured by conduction-electron spin resonance

F. Simon,^{1,2} A. Jánossy,¹ T. Fehér,^{1,2} F. Murányi,¹ S. Garaj,² L. Forró,² C. Petrovic,^{3,*} S. Bud'ko,³ R. A. Ribeiro,³ and P. C. Canfield³

¹*Budapest University of Technology and Economics, Institute of Physics and Solids in Magnetic Fields Research Group of the Hungarian Academy of Sciences, H-1521 Budapest, P.O. Box 91, Hungary*

²*Institute of Physics of Complex Matter, EPFL, CH-1015 Lausanne, Switzerland*

³*Ames Laboratory, U.S. Department of Energy and Department of Physics and Astronomy, Iowa State University, Ames, Iowa 50011, USA*

(Received 1 March 2005; revised manuscript received 2 June 2005; published 22 July 2005)

The magnetic-field dependence of the electron spin susceptibility χ_s was measured in the superconducting state of high-purity MgB_2 fine powders from the intensity of the conduction-electron spin resonance at 3.8, 9.4, and 35 GHz. The measurements confirm that a large part of the density of states is restored at low temperatures at fields below 1 T in qualitative agreement with the closing of the π band gaps in the two-band model. However, the increase of χ_s with field and temperature is larger than expected from current superconductor models of MgB_2 .

DOI: [10.1103/PhysRevB.72.012511](https://doi.org/10.1103/PhysRevB.72.012511)

PACS number(s): 74.70.Ad, 74.25.Ha, 74.25.Nf, 76.30.Pk

It is now generally accepted that MgB_2 is a phonon-mediated superconductor¹⁻³ which owes its unusual properties to the strong differences in the electron-phonon coupling of its disconnected Fermi surface sheets.⁴ The two-gap model assigns a large superconductor gap to the cylindrical Fermi surface sheets originating from B-B σ bonds and a much smaller gap to the sheets of π electrons. The model successfully describes the temperature dependence of several properties like the specific heat⁵ or the electron tunneling spectra⁶ in zero magnetic field while predictions for finite magnetic fields are less tested. The strong electron-phonon coupling on the σ sheets maintains superconductivity to about $H_{c2}^c \approx 2.5$ T for fields perpendicular to and $H_{c2}^{ab} \approx 16$ T for fields lying in the crystalline (a, b) boron planes.⁷ It has been suggested that the weaker π gap is closed by much smaller fields H_{c2}^π without destroying superconductivity. The actual value of H_{c2}^π is rather uncertain: from single-crystal specific heat experiments⁸ an isotropic $H_{c2}^\pi = 0.3-0.4$ T, from vortex imaging⁹ 0.13 T has been estimated, while point contact tunneling experiments¹⁰⁻¹³ suggest values between 1 and 2 T.

In this paper, we report on the magnetic-field dependence of the electron spin susceptibility χ_s in the superconducting state of high-purity MgB_2 powders measured by conduction-electron spin resonance (CESR). We observe an unusually strong increase of χ_s with magnetic field. χ_s at low temperatures measures the density of states (DOS) at the Fermi level restored in the superconductor by the magnetic field. Apart from the weak electron-electron interactions, χ_s is proportional to the DOS in MgB_2 and may be compared to band structure calculations directly or to the electronic specific heat after a correction for electron-phonon coupling. $\chi_s(H, T)$ is not proportional to the electronic specific heat coefficient $\gamma(H, T)$ if the electron-phonon coupling is different for the σ and π bands. We find, however, a larger increase of χ_s with field and temperature than expected from calculations of the DOS and a simple two-band model.

We studied samples from several batches. Sample 1 is made from a 99.99% purity natural isotopic mixture of ^{10}B and ^{11}B amorphous boron; samples 2 and 3 are made from crystalline, isotopically pure ^{11}B . Chemical analysis, the high normal-state conductivities, and the narrow CESR lines at T_c attest to the high purity of the samples. Details of sample characterization are discussed in Ref. 14. Sample 2 was made from the batch used in the CESR work of Ref. 7. Fine powders with grain sizes less than $1 \mu\text{m}$ were selected from the starting materials to reduce the inhomogeneity of microwave excitation. The aggregates of small grains were hand crushed and then mixed in a 1:1 weight ratio with a fine SnO_2 powder. The mixture was suspended in isopropanol and the larger particles were eliminated by sedimentation or in a centrifuge while the small grains were extracted by filtering. Mixing with SnO_2 separates the MgB_2 particles and reduces eddy-current screening of microwaves. We checked by electron microscopy that MgB_2 grains were smaller than $0.5 \mu\text{m}$. Superconducting quantum interference device (SQUID) magnetometry confirmed that the superconducting properties are the same in the original batch and the sample of small grains. The powders were finally cast into epoxy for the ESR experiments. CESR experiments were performed at 3.8, 9.4, 35, 75, and 225 GHz corresponding to approx. 0.14, 0.34, 1.28, 2.7, and 8.1 T resonance fields, respectively. The higher-frequency experiments reproduce those of Ref. 7; the CESRs of superconducting and normal grains are resolved at 75 and 225 GHz even at temperatures much below T_c , confirming that H_{c2}^c is somewhat below 2.7 T. χ_s of MgB_2 was measured directly from the CESR intensity without need for core electron corrections as in static susceptibility measurements. A fine powder of the air-stable metallic polymer $o\text{-KC}_{60}$ was mixed into the epoxy for some of the samples to serve as a temperature-independent ESR intensity standard.¹⁵ Intensity measurements at 9 GHz (where instrumental factors are well controlled) with and without KC_{60} were consistent. The absolute value of χ_s was measured against a secondary $\text{CuSO}_4 \cdot 5\text{H}_2\text{O}$ standard at 9.4 GHz.

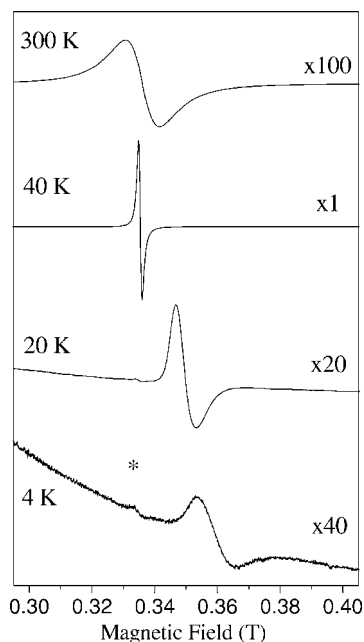


FIG. 1. Temperature dependence of the CESR signal of MgB_2 fine powder sample (sample 1) at 9.4 GHz (0.34 T). * denotes the ESR signal of a tiny amount of paramagnetic impurity phase.

Figure 1 shows the CESR spectra at 9.4 GHz for sample 1. The room-temperature peak-to-peak linewidth $\Delta H_{pp} = 111 \pm 3$ G of the derivative absorption line is dominated by spin-lattice relaxation due to phonons. The residual linewidth at 40 K arises from static imperfections and is sample dependent. The residual linewidth is somewhat smaller for sample 1 ($\Delta H_{pp} = 10 \pm 0.3$ G) than for samples 2 and 3 (11 ± 0.3 and 20 ± 0.6 G), while the residual resistance ratio (RRR) is larger for the latter two samples.¹⁴ Unlike the RRR, the CESR linewidth is insensitive to intergrain scattering and the difference may be related to the different morphology of Sample 1 and 2, 3. The small asymmetry of the line shape (the ratio of maxima of the derivative ESR line $A/B = 1.16$ for sample 1) at 40 K shows that microwave penetration is nearly homogeneous,¹⁶ the typical particle size is comparable to the microwave penetration depth, $\delta = 0.3 \mu\text{m}$, and the reduction of the CESR signal intensity due to eddy-current screening is less than 5%.

Above 450 K (data not shown), the CESR intensities are the same for the three samples and correspond to a susceptibility of $\chi_s = (2.3 \pm 0.3) \times 10^{-5}$ emu/mol in agreement with the previously measured value⁷ of $\chi_s = (2.0 \pm 0.3) \times 10^{-5}$ emu/mol and calculations of the DOS.³ In sample 1, the CESR intensity is nearly T independent in the normal state; the measured small decrease of about 20% between 600 and 40 K is of the order of experimental precision at high temperatures. In samples 2 and 3 the CESR intensity decreased by a factor of 2.5 between 450 and 40 K. The nearly symmetric Lorentzian line shape showed that this intensity decrease is not due to a limited penetration depth. Neither does the intensity decrease correspond to a change in χ_s . We measured the T dependence of the ^{11}B spin-lattice relaxation time T_1 in samples 2 and 3 and found a metallic, T -independent value of $1/(TT_1) = 167 \pm 3 \text{ s}^{-1} \text{ K}^{-1}$ in agree-

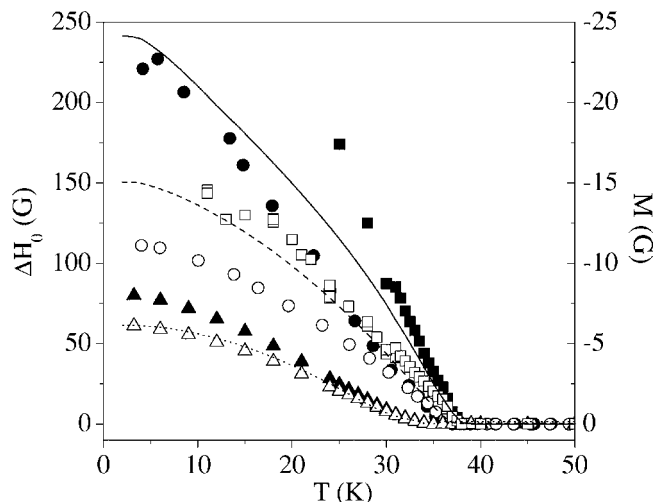


FIG. 2. Temperature dependence of the diamagnetic shift (full symbols are up sweeps, open symbols are down sweeps) of the CESR (squares, 3.8 GHz, 0.14 T; circles, 9.4 GHz, 0.34 T; triangles, 35 GHz, 1.28 T) and diamagnetic magnetization measured by SQUID (solid, dashed, and dotted curves are at 0.14, 0.34, and 1.28 T, respectively).

ment with Refs. 17 and 18. It is possible that the difference in morphology and purity at the grain surfaces explains that the CESR signal intensity is almost constant in sample 1 while it changes strongly in samples 2 and 3. We believe that the nearly constant CESR intensity in sample 1 and the constant $1/(TT_1)$ measures correctly the metallic susceptibility of MgB_2 .

Below T_c , the T and H dependence of the diamagnetic shifts, line widths, and intensities normalized at T_c are similar in all three samples. We discuss sample 1, for which the CESR signal intensity is constant in the normal state within experimental precision. For applied magnetic fields $H < H_{c2}^c(T=0 \text{ K})$ and at $T \ll T_c$ the CESR signal corresponds to the mixed state of the MgB_2 superconductor; any nonsuperconducting fraction would be shifted to higher fields and easily detected.⁷ The ESR of a tiny impurity phase is well outside the CESR of MgB_2 (marked by * in Fig. 1). Comparison of the diamagnetic magnetization M measured by SQUID and the diamagnetic shift of the CESR, $\Delta H_0(T) = H_0(T) - H_0(40 \text{ K})$ (H_0 is the resonance field), also verifies that below T_c we detect the CESR of the MgB_2 superconductor. Figure 2 shows $\Delta H_0(T)$ at three different ESR frequencies and M at the corresponding static magnetic fields with a scaling between ΔH_0 and M as in Ref. 7. The present diamagnetic shift data on fine-grain samples at 35 GHz and higher frequencies (not shown) agree with our previous report on large-grain samples.⁷ $\Delta H_0(T)$ is equal to the average reduction of the applied magnetic field in the sample and is proportional within a shape dependent constant to M of the grains. $\Delta H_0(T)$ averaged for increasing and decreasing field sweeps is proportional to M in the field cooled sample with the same proportionality constant in a broad range of T 's for all the three magnetic fields. We used the same argument previously to identify the CESR of superconducting MgB_2 particles at higher-frequency (> 35 GHz) CESR experiment.⁷

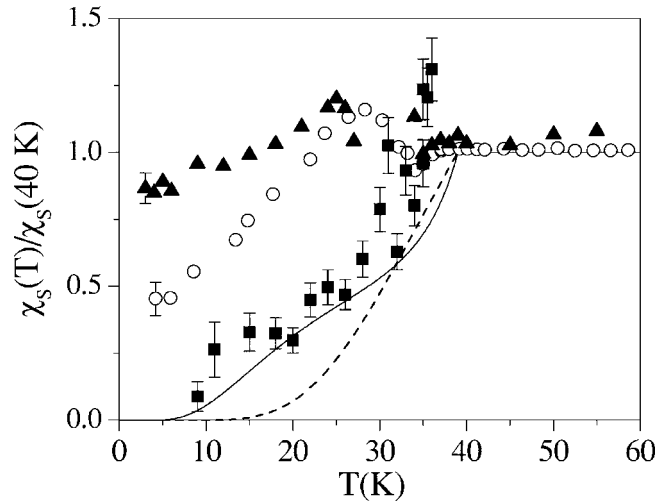


FIG. 3. The temperature- and magnetic-field-dependent spin susceptibility of MgB_2 below T_c (squares, 3.8 GHz, 0.14 T; circles, 9.4 GHz, 0.34 T; triangles, 35 GHz, 1.28 T). Dashed and solid curves are χ_s in the absence of magnetic field as calculated for the isotropic BCS and two-gap models, respectively, as explained in the text.

The CESR line broadens inhomogeneously below T_c due to the macroscopic inhomogeneities of diamagnetic stray fields. Within each isolated grain, spin diffusion motionally averages all magnetic field inhomogeneities arising from screening currents and the vortex lattice,¹⁹ so this itself does not broaden the CESR of the individual grains. The line is, however, broadened in the randomly oriented powder by the crystalline and shape anisotropy of the diamagnetic shift, that changes from grain to grain. As expected for this case, the observed additional line width in the superconducting state, ΔH_a , is proportional to the shift and $\Delta H_a/\Delta H_0(T)$ is about 0.3 at all fields and temperatures.

The main topic of the current report is the measurement of χ_s in the superconducting state of MgB_2 . Usually, χ_s is determined from the measurements of temperature-dependent Knight shift or spin-lattice relaxation time T_1 .²⁰ To our knowledge, in MgB_2 there has been no successful determination of these quantities below T_c : precision of the Knight shift measurement is limited due to the diamagnetic magnetization,^{17,21} while T_1 measurements are affected by several factors like vortex motion.¹⁷ In CESR, the signal intensity is proportional to χ_s and diamagnetism affects only the shift of the resonance line. χ_s is proportional to the DOS of low-energy quasiparticle excitations when electron correlations are small.

In Fig. 3, we show χ_s below 60 K measured at three magnetic fields. The 9.4 GHz (0.34 T) and 35 GHz (1.28 T) data are normalized at 40 K while the 3.8 GHz (0.14 T) data are normalized at 100 K. At 3.8 and 35 GHz data are missing in ranges between 36 and 100 K and 27 and 34 K, respectively, where the CESR of MgB_2 could not be resolved from the KC_{60} reference. Data taken at 9.4 GHz with and without reference agree well. Hysteresis in the penetration of the magnetic field into the sample below the irreversibility line does not affect the measurement of χ_s in the studied range of T

and H : line widths and shifts depend on the direction of the field sweep at low T but the intensities are the same within 5%, i.e., within the experimental precision at low T . In Fig. 3, data at 9.4 and 35 GHz are averaged for sweeps with increasing and decreasing fields while at 3.8 GHz decreasing field sweep data are shown. No correction is made for diamagnetic screening of the microwave excitation; this would increase somewhat further the measured values of χ_s .

The remarkably fast increase of χ_s with field and temperature is the most interesting finding of this work. As shown in Fig. 3, the data cannot be described by a superconductor with a single gap. The T -dependent χ_s at our lowest magnetic field of 0.14 T lies well above $\chi_s(T, H=0)$ calculated for an isotropic $T_c=39$ K weak-coupling superconductor.²²⁻²⁴ In a conventional superconductor a field of 0.14 T would affect the spin susceptibility little since H_{c2} varies between 2.5 and 16 T.

As we show below, the two-gap model is more successful: it explains data at the lowest field, but difficulties remain with the interpretation of data at higher fields. The solid curve in Fig. 3 shows χ_s calculated for zero field in a model of two independent zero-temperature gaps $\Delta_1=11$ K and $\Delta_2=45$ K. (These values are derived from zero-field specific heat⁸ and electron tunneling data.¹⁰) Following band structure calculations,^{4,26,27} we assumed that N , the total DOS in the normal state, is shared in a ratio $N_{\pi_0}/N_0=0.56$ and $N_{\sigma_0}/N_0=0.44$ between the two types of Fermi surfaces.²⁵ Clearly, χ_s measured at 0.14 T and above 10 K is compatible with the two-gap model using the above parameters without any important enhancement of χ_s by the field.

The large susceptibilities at the fields of 0.34 and 1.28 T are, however, only in qualitative agreement with the two-gap model. These fields are still much below the critical field for destroying superconductivity. The explanation for the strong magnetic-field dependence observed in various experiments has been that the gap in the type- π band is closed by fields of 1 T or less, i.e., by fields much below H_{c2} . In this picture the DOS $N(H)=N_{\pi}+N_{\sigma}$ increases rapidly with field until H_{c2}^{π} , where the contribution of the π band to the DOS saturates at the normal-state value N_{π_0} . At fields above H_{c2}^{π} , the increase of $N(H)$ is much slower as it arises solely from the σ band and H_{c2} is much larger than H_{c2}^{π} for all field orientations. Figure 4 shows the DOS calculated in the simplest approximation, where both N_{π} and N_{σ} increase linearly with field until they reach their normal-state value at H_{c2}^{π} and H_{c2} . The experimental density of states [proportional to $\chi_s(H)$] follows such a nearly steplike behavior, in agreement with an H_{c2}^{π} equal to or less than 1 T. However, the susceptibility $\chi_s/\chi_N=0.87(6)$ measured at 1.28 T and 4 K is much larger than expected. Extrapolating to zero field, the susceptibility predicts $N_{\pi_0}/N_0|_{\chi}=0.8-0.9$, a value much larger than $N_{\pi_0}/N_0=0.56$ calculated by several groups.

We note that the magnetic-field dependence of the electronic specific heat is not in perfect agreement with the band structure calculations, either. Specific heat experiments on MgB_2 single crystals in magnetic field yield an isotropic critical field $H_{c2}^{\pi}=0.4$ T and $\gamma_{\sigma}/\gamma=0.45$ and $\gamma_{\pi}/\gamma=0.55$ for the electronic specific heats of the two bands in the normal states.⁸ While electron-phonon coupling does

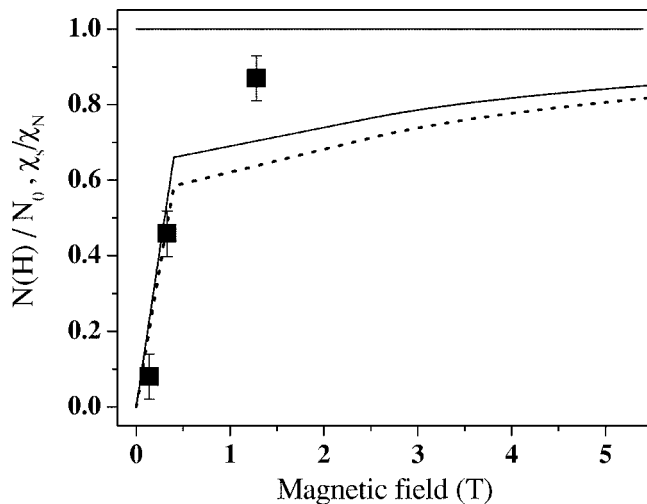


FIG. 4. Comparison of the measured field dependence of the low-temperature normalized susceptibility χ_s/χ_N (squares) to the predictions of the two-gap model of Ref. 26. The magnetic-field-dependent DOS (dashed line) is assumed to have independent contributions from a π band with $H_{c2}^\pi=0.4$ T and a σ band with $H_{c2}^\sigma=2.5$ T and $H_{c2}^{ab}=16$ T. The solid line represents DOS calculated from single-crystal specific heat measurements (Ref. 8).

not affect the spin susceptibility, it contributes to γ by a factor of $1+\lambda$. Thus the DOS calculated from the heat capacity is $N_{\pi 0}/N_0=[\gamma_\pi/(1+\lambda_\pi)]/[\gamma_\pi/(1+\lambda_\pi)+\gamma_\sigma/(1+\lambda_\sigma)]$ and $N_{\sigma 0}/N_0=[\gamma_\sigma/(1+\lambda_\sigma)]/[\gamma_\pi/(1+\lambda_\pi)+\gamma_\sigma/(1+\lambda_\sigma)]$. Using the theoretical values of the electron-phonon coupling constants, $\lambda_\pi=0.4$ and $\lambda_\sigma=0.9$,²⁵ yields $N_{\pi 0}/N_0|_{\gamma}=0.62$, which is less than that measured from the spin susceptibility but still significantly larger than the calculated value of 0.56.

The DOS from the band structure calculations is probably reliable; it describes the zero-field specific heat correctly. The

same calculations predict electron-phonon couplings that are in agreement with the experiments.²⁸ Thus, we conclude that a magnetic field of about 1 T does not simply close the π band gap but it restores also a large portion of the Fermi surface on the σ band. This conclusion is reinforced by the observed temperature dependence at 0.34 T. Although χ_s measured at 0.34 T and 4 K may agree with a two-gap model with negligible perturbation of the σ band by small magnetic fields, there is an unexpectedly large effect of the magnetic field at higher temperatures. Most of the spin susceptibility is restored at $T_c/2$ by a field of 0.34 T. It is evident that such a large spin susceptibility cannot be explained by a simple picture where the π band gap is closed at fields below 1 T and the σ band DOS is restored only at a rate proportional to H/H_{c2} .

In conclusion, the strong magnetic-field dependence of the spin susceptibility and specific heat poses a challenge to theory. The model where the π gap is closed at small fields while the σ gap remains mostly unaffected is inadequate.

Support from the Hungarian State Grant Nos. OTKA T029150, OTKA TS040878, and FKFP 0352/1997 and the Swiss National Science Foundation and its NCCR “MANEP” are acknowledged. We are indebted to M. Horvatić for his contribution to the ¹¹B NMR experiments. The authors are grateful to Silvija Gradečak and Csilla Mikó for the scanning electron microscopy experiments and to Edina Couteau for assistance in the fine-powder preparation. F.S. and T.F. acknowledge the Bolyai Hungarian Research Foundation and F.S. acknowledges the Magyary Grant Programme for support. T.F. acknowledges the hospitality of the Grenoble High Magnetic Field Laboratory during the NMR measurements. Ames Laboratory is operated for the U.S. Department of Energy by Iowa State University under Contract No. W-7405-Eng-82.

*Present address: Department of Physics, Brookhaven National Laboratory, Upton, New York 11973.

¹J. Nagamatsu *et al.*, Nature (London) **410**, 63 (2001).

²S. L. Bud'ko *et al.*, Phys. Rev. Lett. **86**, 1877 (2001).

³J. Kortus *et al.*, Phys. Rev. Lett. **86**, 4656 (2001).

⁴A. Y. Liu, I. I. Mazin, and J. Kortus, Phys. Rev. Lett. **87**, 087005 (2001).

⁵F. Bouquet *et al.*, Phys. Rev. Lett. **87**, 047001 (2001).

⁶P. Szabó *et al.*, Phys. Rev. Lett. **87**, 137005 (2001).

⁷F. Simon *et al.*, Phys. Rev. Lett. **87**, 047002 (2001).

⁸F. Bouquet *et al.*, Phys. Rev. Lett. **89**, 257001 (2002).

⁹M. R. Eskildsen *et al.*, Phys. Rev. Lett. **89**, 187003 (2002).

¹⁰R. S. Gonnelli *et al.*, Phys. Rev. Lett. **89**, 247004 (2002).

¹¹P. Samuely *et al.*, Physica C **385**, 244 (2003).

¹²S. L. Bud'ko, V. G. Kogan, and P. C. Canfield, Phys. Rev. B **64**, 180506(R) (2001).

¹³S. L. Bud'ko and P. C. Canfield, Phys. Rev. B **65**, 212501 (2002).

¹⁴R. A. Ribeiro *et al.*, Physica C **382**, 194 (2002).

¹⁵F. Bommeli *et al.*, Phys. Rev. B **51**, 14794 (1995).

¹⁶F. J. Dyson, Phys. Rev. **98**, 349 (1955).

¹⁷J. K. Jung *et al.*, Phys. Rev. B **64**, 012514 (2001).

¹⁸H. Kotegawa *et al.*, Phys. Rev. Lett. **87**, 127001 (2001).

¹⁹P. G. de Gennes, Solid State Commun. **4**, 95 (1966).

²⁰C. P. Slichter, *Principles of Magnetic Resonance* (Springer-Verlag, New York, 1990).

²¹A. P. Gerashenko *et al.*, Appl. Magn. Reson. **21**, 157 (2001).

²²Kei Yosida, Phys. Rev. **110**, 769 (1958).

²³F. Bouquet *et al.*, Europhys. Lett. **56**, 856 (2001).

²⁴A. Junod *et al.*, cond-mat/0106394 (unpublished); F. Bouquet *et al.*, Physica C **385**, 192 (2003).

²⁵H. J. Choi, M. L. Cohen, and S. G. Louie, Physica C **385**, 66 (2003).

²⁶H. J. Choi *et al.*, Nature (London) **418**, 758 (2002).

²⁷A. A. Golubov *et al.*, J. Phys.: Condens. Matter **14**, 1353 (2002).

²⁸A. Carrington *et al.*, Phys. Rev. Lett. **91**, 037003 (2003).